

## VOLTAGE CONTROL OF DISTRIBUTION NETWORKS WITH PHOTOVOLTAIC POWER SOURCES

Jan Veleba

### **ABSTRACT**

*This paper deals with voltage control of distribution networks with high representation of photovoltaic power sources. To simulate this, modified IEEE 123-bus radial power system has been equipped with time-dependent loads and generations from PV power plants to include various loading and voltage scenarios of the system. For voltage control, operations of load tap-changing transformers (LTCs) connected to both HV and MV voltage levels have been simulated using traditional Gauss-Seidel method. Multiple load flow calculations along with voltage control algorithms for LTCs were performed in Matlab environment.*

### **1. INTRODUCTION**

Until recently, Czech distribution networks have been operated as standard radial systems with electric power delivery from superior power grids. No other power sources, except of relatively small power plants e.g. in factories, were connected on MV and LV voltage levels. The operation of such networks was strongly influenced only by high inter-tie flows from the HV side. This significantly facilitated the entire voltage control of the network. The superior HV/MV transformer was equipped by an under-load tap changer to provide relatively smooth voltage regulation on its secondary side. In case of more MV voltage levels situated in such distribution network, relevant MV/MV or MV/LV transformers were installed with the possibility of variable tap setting in an open state only. On the customer side, permitted voltages were ensured by means of rather rough tap steps of these transformers.

In last several years, new energy policies and developments (especially installations of renewable or other dispersed power sources) seriously changed the principles of network operation and control. However, from the voltage point of view, control mechanisms were affected only slightly and in critical cases the voltage problems were solved by means of static shunt compensators.

In future smart grids and other islanded systems, voltage control will play the most important role for keeping voltages on consumption side within the limits. For this, perfect co-operation of broad variety of devices – LTC transformers, switched shunt capacitors, synchronous compensators, etc. - will have to be used even on the MV side of the system.

### **2. MODELLING OF LTC TRANSFORMERS IN THE GAUSS-SEIDEL METHOD**

Despite of relatively obsolete (but functional and highly reliable) numerical principle, the Gauss-Seidel can be used for providing load flow solutions of even larger power systems. For these and also when performing load flow studies of distribution networks, higher number of iterations are needed to obtain sufficient level of convergence. In latter case, the reason is caused by high R/X ratios of network branches, radial system topology and large differences in lengths of individual

overhead/cable lines. However, when combined with suitably adjusted acceleration techniques, numbers of iterations can be significantly reduced and even more complicated simulations such as modelling of var limits for PV buses or inclusion of LTC transformers can be successfully realized.

For each numerical load flow method, different algorithm must be chosen for respecting its own physical nature and thus allowing its best numerical performance. For the G-S method, the chosen LTC algorithm for voltage control [1] is as follows.

1] The calculation is started with initial tap magnitudes.

2] If pre-set convergence level obtained, new numbers of tap step positions are computed directly. Symbol 'R' denotes the rounding process to the closest integer.

$$n_{t_{ik}} = \left[ \frac{V_m^{(p)} - V_m^{sp}}{V_m^{(p)} \Delta t_{ik}} \right]^R \quad (1)$$

where:  $V_m^{(p)} - V_m^{sp}$  is the voltage error between currently calculated voltage magnitude and the targeted voltage value, respectively

$\Delta t_{ik}$  is the tap step of the LTC transformer

3] New tap setting for voltage control is calculated.

$$t_{ik}^{(p+1)} = t_{ik}^{(p)} + n_{t_{ik}} \Delta t_{ik} \quad (2)$$

Note: Formula (2) corresponds with such equivalent scheme of the transformer, where the tap ratio is regulated on its "primary" side, while the  $\Pi$ -element is on its "secondary" side. In another words, to increase the secondary voltage, the taps must be decreased.

4] Tap corrections must be performed with respect to possibly exceeded tap limits.

$$t^{(p+1)} = \begin{cases} t^{\max} & \text{if } t^{(p+1)} > t^{\max} \\ t^{\min} & \text{if } t^{(p+1)} < t^{\min} \end{cases} \quad (3)$$

5] Bus admittance matrix is modified due to changed taps, the new iteration begins.

If the tap limit is exceeded for more LTC transformers in that particular iteration, only the transformer with the greatest tap error is permanently switched to fixed mode with its tap value adjusted to the exceeded limit.

Modelling of LTC transformers is a discrete simulation. Therefore, the degree of freedom is increased and multiple generally correct solutions can be obtained. Among these solutions, the solution with the lowest total voltage error should be taken as the best available solution.

The problem is also when the value of denominator in (1) is getting significantly larger than of the numerator, rounding process can find no change in taps in the particular iteration, even if the voltage error is still relatively high. Then, proper corrections of the algorithm above must be accomplished to prevent this situation to occur.

Another difficulty is connected with iterative oscillations of LTC transformers between usually two tap settings because none of them provide satisfiable voltage magnitude when compared to respective voltage target. In such a case, only a limited number of "jumps" between two tap settings can be allowed, otherwise the tap ratio leading to smaller target voltage proximity is selected and such transformer is permanently switched to unregulated one.

From above, problems with LTC modelling in the G-S method can be serious. They cannot be seen in advance from the presented algorithm, but only from multiple simulations of reliable load flow scenarios. Therefore, the level of robustness of such algorithm rests fully with the knowledge, experience and skills of the programmer.

### 3. MODELLING OF PHOTOVOLTAIC POWER PLANTS

Photovoltaic power plant is usually modelled by an equivalent circuit with current source  $I_{ph}$  (see Fig. 1). This current represents the generation of the photovoltaic cell and is directly proportional to solar radiation. In the scheme, both diode and resistance  $R_S$  are also situated. Element  $R_S$  represents

the resistance of the cell and of connections between the cells, output current  $I$  flows through it to the network.

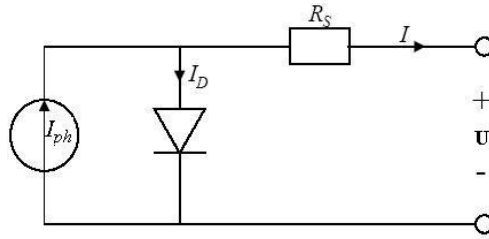


Figure 1 – Equivalent model of the photovoltaic system [2]

Important graphical representation of the photovoltaic cell is the V-A characteristic - see Fig. 2. Maximum current and voltage, whose the cell can theoretically achieve, are the short-circuit current and no-load voltage. Both these values, along with maximum output power are provided by the manufacturer.

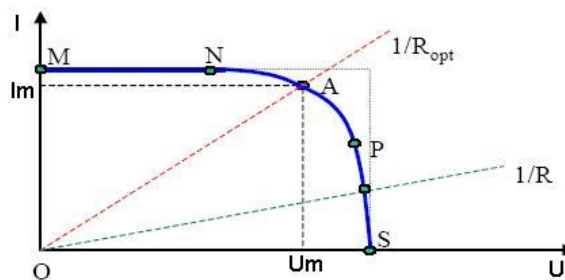


Figure 2 – V-A characteristic of the photovoltaic cell [2]

The cell can produce various number of output powers for individual combinations of currents and voltages. Maximum output power is the one with the highest product of current and voltage - point A. Such optimum current and voltage is also recorded in the manufacturer's catalogue, but these values (among others) correspond only to the optimum testing lab conditions such as reference temperature  $t_{C0}$  and reference irradiation  $G_{a0}$ , optimum radiation spectrum, etc. Therefore, the V-A characteristic is not fixed in everyday operation, but variable especially with current temperature and solar irradiation. Then, the DC-AC converter must track the optimum voltage, for which the cell generates the maximum power output and thus it has the maximum efficiency. The effect of solar irradiance and temperature of the cell are shown in Figs. 3a,b.

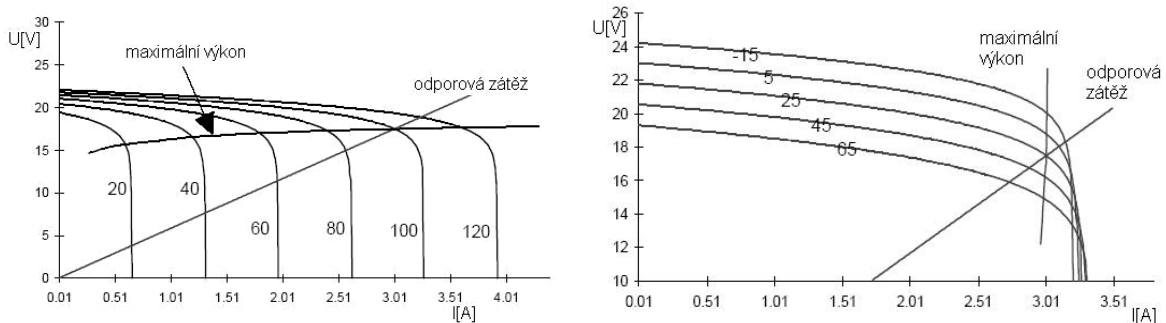


Figure 3a – Effect of solar irradiance [ $\text{W/m}^2 \times 0.1$ ] on the V-A characteristic [2]

Figure 3b – Effect of temperature of the cell [ $^{\circ}\text{C}$ ] on the V-A characteristic [2]

As can be seen, both these effects strongly influence power generation of a solar cell. Therefore, proper steady-state model of the cell [2] should contain not only equation describing its V-A characteristics but also relevant corrections for both these factors.

The V-A characteristic of the solar cell, i.e. dependence of current  $I$  on voltage  $U$ , is as follows:

$$I = I_{SC} \left[ 1 - e^{-\frac{U-U_{OC}}{mU_t}} \right] \quad (4)$$

where:  $I_{SC}$  short-circuit current with irradiance and temperature correction  
 $U_{OC}$  no-load voltage with irradiance and temperature correction  
 $U_t$  thermal voltage varying according to the cell's temperature  
 $m$  idealizing factor [-]

Correction of the short-circuit current is:

$$I_{SC} = C_1 G_a + K_1 (T^C - T^{C0}) \quad (5)$$

where:  $C_1$  material (nameplate) constant of the cell [ $\text{Am}^2/\text{W}$ ]  
 $K_1$  material (nameplate) constant of the cell [ $\text{A/K}$ ]  
 $G_a$  actual solar irradiance [ $\text{W/m}^2$ ]  
 $T_C$  thermodynamic temperature [ $\text{K}$ ]  
 $T_{C0}$  reference thermodynamic temperature:  $T^{C0} = 273.15 + t^{C0}$  [ $\text{K};^\circ\text{C}$ ]

Temperature  $T_C$  is computed from ambient temperature  $t_a$  [ $^\circ\text{C}$ ] and irradiance (coefficient  $C_2$  [ $\text{Km}^2/\text{W}$ ]):

$$T^C = t_a + 273.15 + C_2 G_a \quad (6)$$

Correction of the no-load voltage is:

$$U_{OC} = U_{OC0} + C_3 (T^C - T^{C0}) - \frac{1}{K_4} e^{\frac{G_a - G_{a0}}{K_3}} \quad (7)$$

where:  $U_{OC0}$  reference no-load voltage  
 $C_3$  material (nameplate) constant of the cell [ $\text{V/K}$ ]  
 $K_3$  material (nameplate) constant of the cell [ $\log(\text{W/m}^2\text{V})$ ]  
 $K_4$  material (nameplate) constant of the cell [ $\text{W/m}^2\text{V}$ ]

Thermal voltage  $U_t$  is calculated as follows:

$$U_t = \frac{kT^C}{e} \quad (8)$$

where:  $k$  Boltzman's constant ( $k = 1.381 \cdot 10^{-23}$  J/K)  
 $e$  constant for electrical charge ( $e = 1.602 \cdot 10^{-19}$  C)

With respect to actual irradiance and ambient temperature, active power output of the plant is:

$$P = (100 - l) p U I_{SC} \left[ 1 - e^{-\frac{U-U_{OC}}{mU_t}} \right] \quad (9)$$

where:  $p$  total number of photovoltaic cells of the power plant  
 $l$  losses of the power plant

The losses are approx. 2.9 - 3.2% due to angular reflectance and 10 - 13% due to losses on the cables, DC/AC converter and the transformer. To include the behaviour of the DC/AC converter, optimum voltage for current operating state must be found. This is done by differentiating equation (9) and setting to zero. Process leads to a nonlinear equation which can be solved by the Newton method.

Some material constants are given in the manufacturer's catalogue, some can be found in the literature. Typical values are:  $C_1 = 0.00317$  [ $\text{Am}^2/\text{W}$ ],  $C_2 = 0.028$  [ $\text{Km}^2/\text{W}$ ],  $C_3 = -0.0023$  [ $\text{V/K}$ ],  $K_1 = 0.00125$  [ $\text{A/K}$ ],  $K_3 = 300$  [ $\log(\text{W/m}^2\text{V})$ ],  $K_4 = 140$  [ $\text{W/m}^2\text{V}$ ],  $m = 2.5$ .

Cloudiness strongly influences active generation of the photovoltaic power plant -see Fig. 4. Therefore, cloudiness data should be also included to the simulation of the power plant.

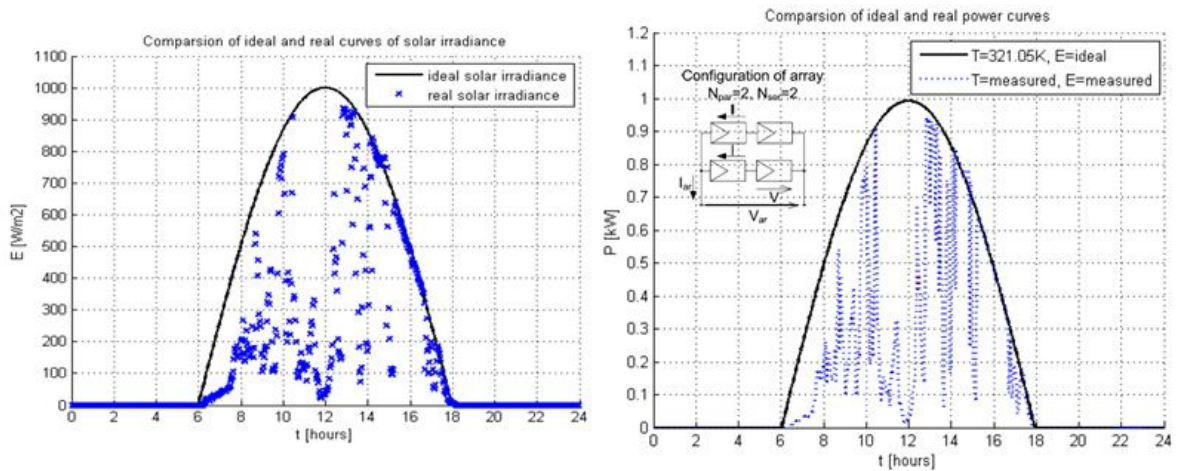


Figure 4 – Effect of cloudiness on active power generation of the power plant [3]

Small photovoltaic power plants up to hundreds of kilowatts can be suitably modelled as PQ power sources. Then, the power factor is not constant but dependent on the irradiance/active power generation. For small irradiance, the reactive power is negative and power plant is consuming reactive power. For higher irradiances, the reactive power becomes positive and delivered to the network by the power plant - see Fig. 5. Note: Authors in [4] used reversed sense of reactive power - negative for generated, positive for consumed.

Large photovoltaic power plants are usually modelled as PV sources, where active power is calculated using the above described DC model and the voltage is kept constant on the optimal value (maintained by the DC/AC converter for maximum power and efficiency). This principle is realized against the reactive power which must be always within its limits. Lower/upper var limits are not constant, but variable depending on generated active power.

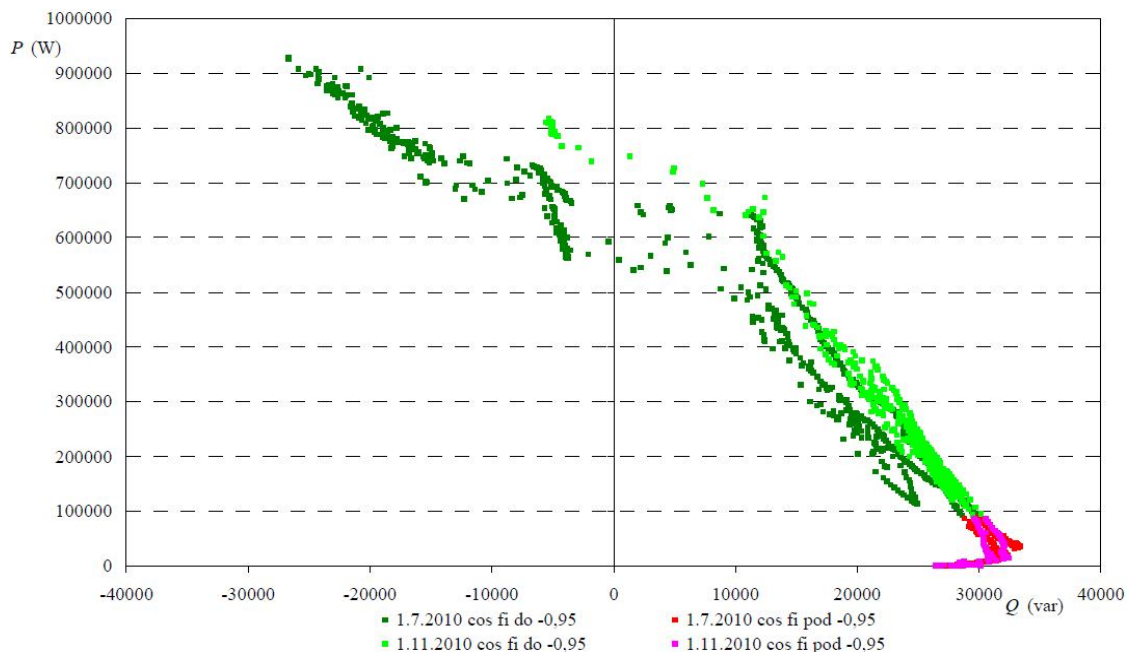


Figure 5 – P-Q diagram of the photovoltaic power plant 1100 kWp [4]

From the P-Q diagram above is obvious, that dependence  $P = f(Q)$  can be easily obtained using a linear function. To do so, for each photovoltaic power plant corresponding var limits should be known or at least estimated.

#### 4. CASE STUDY - PREPARING THE INPUT DATA

To comprehensively evaluate the performance of algorithms for LTC transformers in the Gauss-Seidel method, sufficiently large distribution power system (the IEEE 123-bus radial network) has been chosen - see Fig. 6.

Original three-phase input data (loads, capacitors, passive branch parameters) have been averaged for only one-phase analysis; the switches were opened/closed according to instructions in [5].

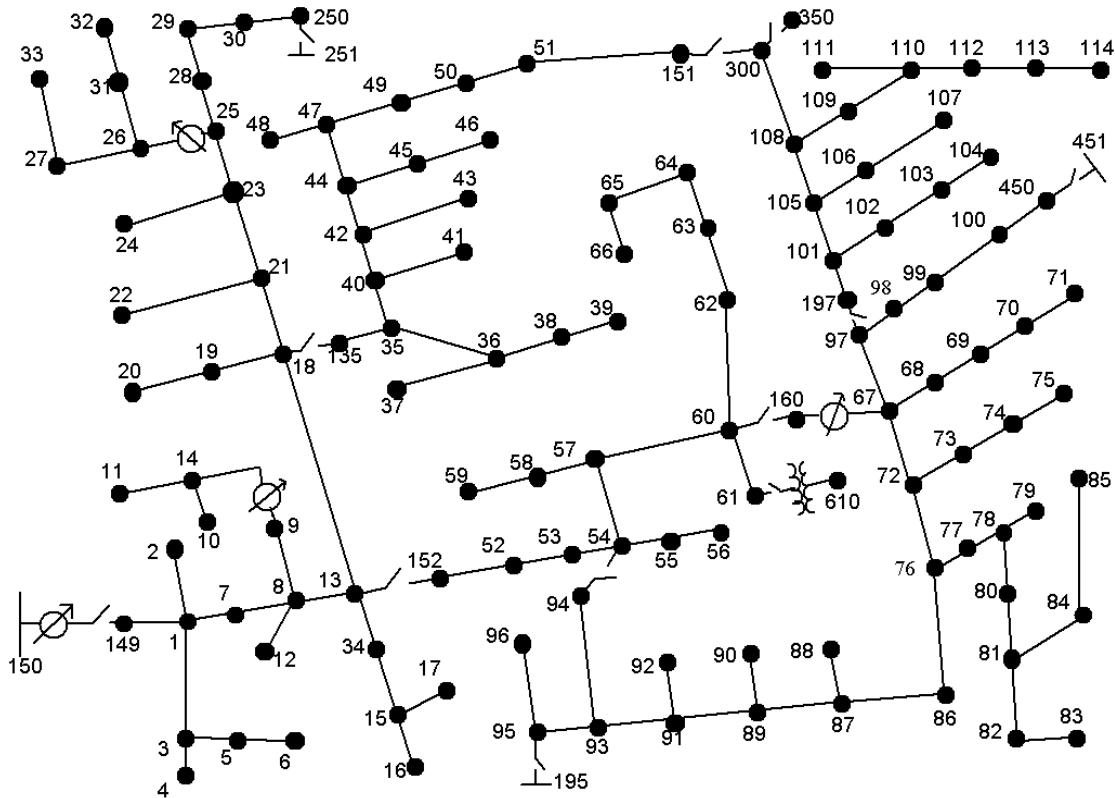


Figure 6 – The IEEE 123-bus radial network - original topology and contents [5]

The network itself contains 115 kV level (bus No. 115, slack bus), 4.16 kV and 0.48 kV (bus No. 610) levels. Main transformer (btw. 150-149) has nominal power 5 MVA, lower transformer 4.16/0.48 kV only 150 kVA. Because of no loads in buses 251, 350, 451, 610 and 195, the 4.16/0.48kV transformers (fixed tap settings) have been placed also to these buses and photovoltaic power plants of 90, 30, 80, 70 and 50 kWp have been connected to these buses, respectively. To include also the possibility of controlling the voltage even on MV voltage level, five extra LTC (4.16/4.16) transformers for voltage control have been placed btw. buses No. 13-152 (nominal power of 3 MVA), 18-21, 18-135, 60-180 and 97-197 (all 2 MVA). For voltage control, tap limits of 0.9 and 1.1 pu with tap step 0.00625 pu (total 33 tap positions, usual in US) have been considered. In all simulations, the secondary bus of each LTC transformer has been selected for voltage control. Finally, the buses have been re-numbered to have buses only between No. 1 and No. 129.

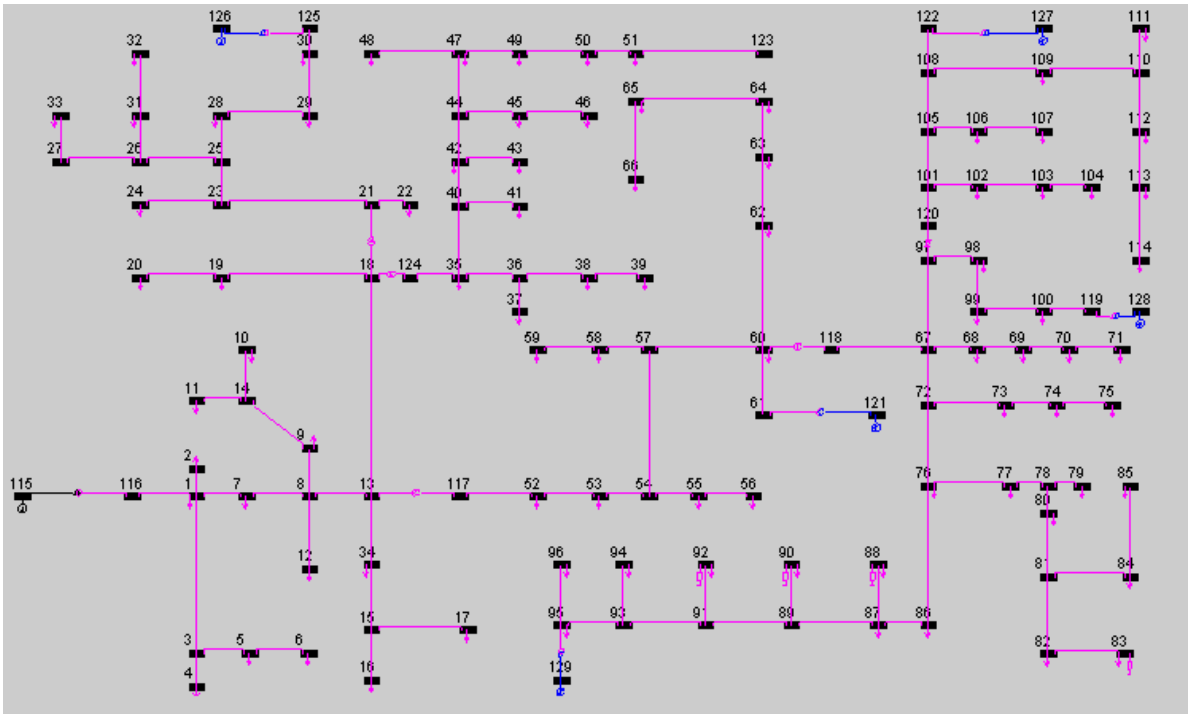


Figure 7 – The IEEE 123-bus radial network - modified and re-numbered

As shown, temperature and irradiance data are crucial for modelling of photovoltaic power plants. To receive this data, specialized web application [6] has been used - see Fig. 8.

Figure 8 – Web application for obtaining irradiance and temperature data for given locality [6]

For given locality (defined by entering its GPS code), chosen month and peak power output of the power plant, average global irradiance and daytime temperature data can be obtained in 15-minute intervals based on long-term satellite measurements. By applying the photovoltaic model

from Chapter 3, previously performed simulations shown the maximum/minimum power generation for the chosen locality (town Maňovice, south-east of Pilsen, CZ) in April and December, respectively. From voltage point of view, irradiance/temperature conditions in April are not important because the bus voltages in the tested network (modified IEEE 123-bus system) are being improved by increased generation from solar plants. On the other hand, data for December respected the most critical voltage conditions in the examined network that may arise due to low active power generations along with large reactive power consumptions. In Fig. 9, table of irradiances and temperatures (columns 1 and 4) for December, generated by online tool [6], are shown. From these data, power coefficients multiplying the peak power of each power plant can be found in an average day of December. Maximum power coefficient value of 0.13361 was found at 12:25 at given locality for month December.

Average Daily Solar Irradiance				
PVGIS Estimates of average daily profiles				
Results for: December				
Solar radiation database used: PVGIS-classic				
Inclination of plane: 35 deg.				
Orientation (azimuth) of plane: 0 deg.				
Time	$G$	$G_d$	$G_e$	$T_d$
06:07	0	0	0	-2.0
06:22	0	0	0	-1.9
06:37	0	0	0	-1.9
06:52	0	0	0	-1.8
07:07	0	0	0	-1.7
07:22	0	0	0	-1.6
07:37	0	0	0	-1.6
07:52	0	0	0	-1.5
08:07	0	0	0	-1.4
08:22	36	22	138	-1.3
08:37	51	30	207	-1.3
08:52	66	38	280	-1.2
09:07	82	46	357	-1.1
09:22	94	51	419	-1.0
09:37	106	56	476	-0.9
09:52	116	61	528	-0.9
10:07	125	64	576	-0.8
10:22	133	68	619	-0.7
10:37	140	71	656	-0.6
10:52	146	73	689	-0.6
11:07	152	75	716	-0.5
11:22	156	77	738	-0.4
11:37	159	78	754	-0.4
11:52	161	79	765	-0.3
12:07	162	79	771	-0.3
12:22	162	79	771	-0.2
12:37	161	79	765	-0.2
12:52	159	78	754	-0.1
13:07	156	77	738	-0.1
13:22	152	75	716	-0.1
13:37	146	73	689	-0.0
13:52	140	71	656	0.0
14:07	133	68	619	0.0
14:22	125	64	576	0.0
14:37	116	61	528	0.0
14:52	106	56	476	0.0
15:07	94	51	419	0.0
15:22	82	46	357	0.0
15:37	66	38	280	-0.0
15:52	51	30	207	-0.0
16:07	19	19	12	-0.1
16:22	0	0	0	-0.1
16:37	0	0	0	-0.2
16:52	0	0	0	-0.2
17:07	0	0	0	-0.3
17:22	0	0	0	-0.4
17:37	0	0	0	-0.5
17:52	0	0	0	-0.6
18:07	0	0	0	-0.7
18:22	0	0	0	-0.8
18:37	0	0	0	-0.9
18:52	0	0	0	-1.1
19:07	0	0	0	-1.2
19:22	0	0	0	-1.4
19:37	0	0	0	-1.6
19:52	0	0	0	-1.7

Figure 9 – Average irradiance and temperature data for given locality and month [6]

For modelling time-dependent loads in individual network buses, original input active and reactive power loads have been taken as maximum (peak) loads. As for photovoltaic power plants, power coefficients (identical for both active and reactive powers) have been applied. These were given as load types (TDD 1-7, normalized load diagrams in one-hour intervals) by [7], and were randomly assigned to individual buses of the examined power system - see Fig. 10.



Figure 10 – Normalized load diagrams for chosen month and day [7]

For having more smooth outputs of the simulation, time-dependent loads and generations from photovoltaic power plants in the network (or better say relevant power coefficients) have been linearly approximated for having 5-minute interval data. In this time region, operation of the system can be still considered as steady-state since all transients would be sufficiently damped through each time interval due to very short time constant of the network.

## 5. CASE STUDY - SIMULATIONS AND RESULTS

In the first simulation, standard operation of the network with nominal voltage in the slack bus has been studied. For this case, no voltage control has been considered. As can be seen from Fig. 11, voltage conditions in some network buses were not maintained inside  $\pm 10\%$  tolerance region in all time intervals. This was definitely caused by very long distances of some branches and buses from the slack bus and by very small power generations from photovoltaic power plants. During the entire simulation, loadings of the 115/4.16 kV and all 4.16/4.16 kV transformers were kept in tolerable margins. Total active power losses were at maximum slightly less than 6 percent. From the numerical point of view, total CPU time needed for calculating all 277 time steps was about 14 minutes. The first case was launched with flat start, remaining time steps with final voltages from previous simulation. Therefore, total number of iterations in individual time steps has been significantly reduced. Highly effective acceleration technique for speeding-up the performance of the G-S method was also applied, which decreased the number of iterations in all time intervals below 1,200 iterations. Without this technique, the entire simulation would be entirely impossible.

In the second simulation, only the 115/4.16 kV transformer has been activated for controlling the secondary bus voltage on value 1.05 pu through all time intervals. Primary voltage was maintained at nominal value. Here can be seen, that it was possible to maintain all network voltages within their permitted limits using this LTC transformer. This is not surprising since this is the way how today's distribution networks are operated. Because of tap switchings, numbers of iterations were significantly increased up to 12,000 - 14,000 iterations in some cases. Therefore, the CPU time needed for this calculation was approx. 25 minutes.

In the third simulation, significantly worse voltage conditions in the superior power system have been set, i.e. voltage magnitude in the slack bus was lowered to 0.92 pu. This situation can be typical in today's power systems, which are operated close to their feasible limits resulting in significant voltage drops across the transmission network and seriously endangered voltage stability. The 115/4.16 kV transformer was again set to be voltage-regulated with target secondary voltage 1.1 pu. From Fig. 13 is visible, that there was no tap switching throughout the entire observed time period. The transformer switched its tap to the minimum value (0.9 pu) and it was still not able to reach the target voltage. More importantly, from the voltage graph it is obvious, that this usual mechanism did not lead to keep network voltages within their permitted limits.

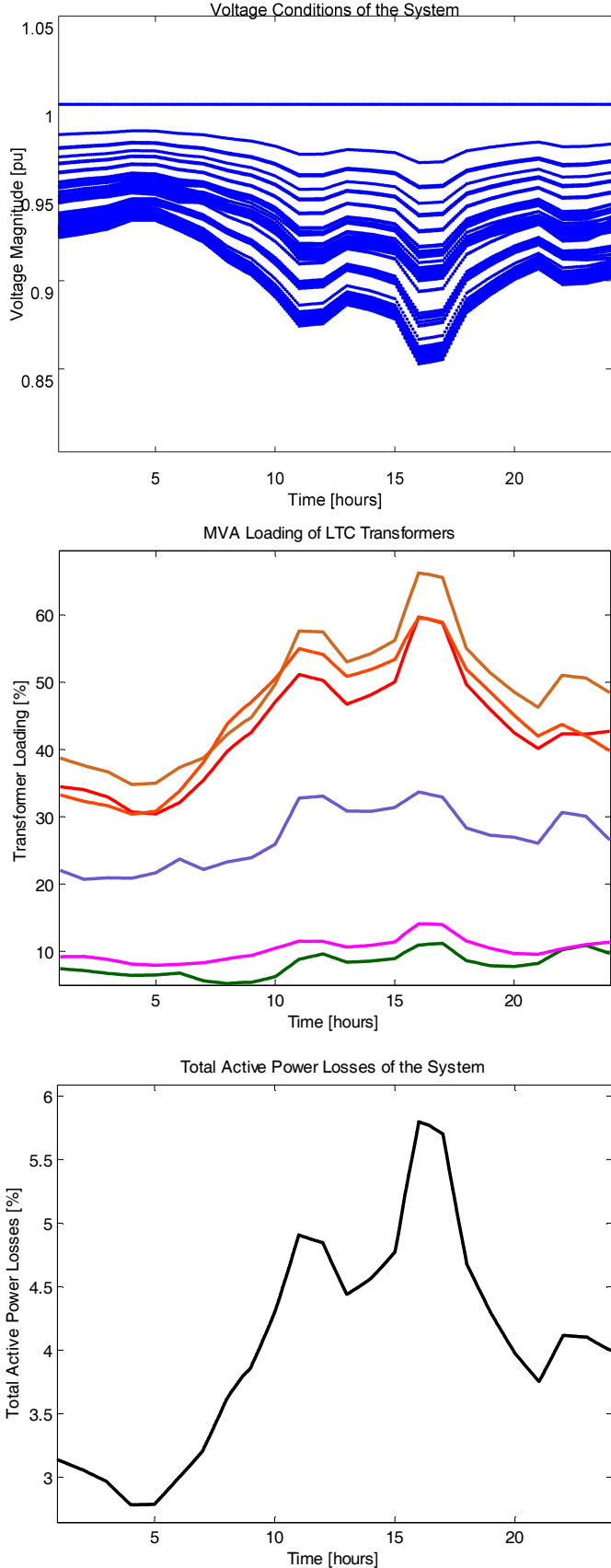


Figure 11 – Standard operation of the system - no voltage control: voltage conditions, HV/MV and MV/MV transformer loadings, total active power losses

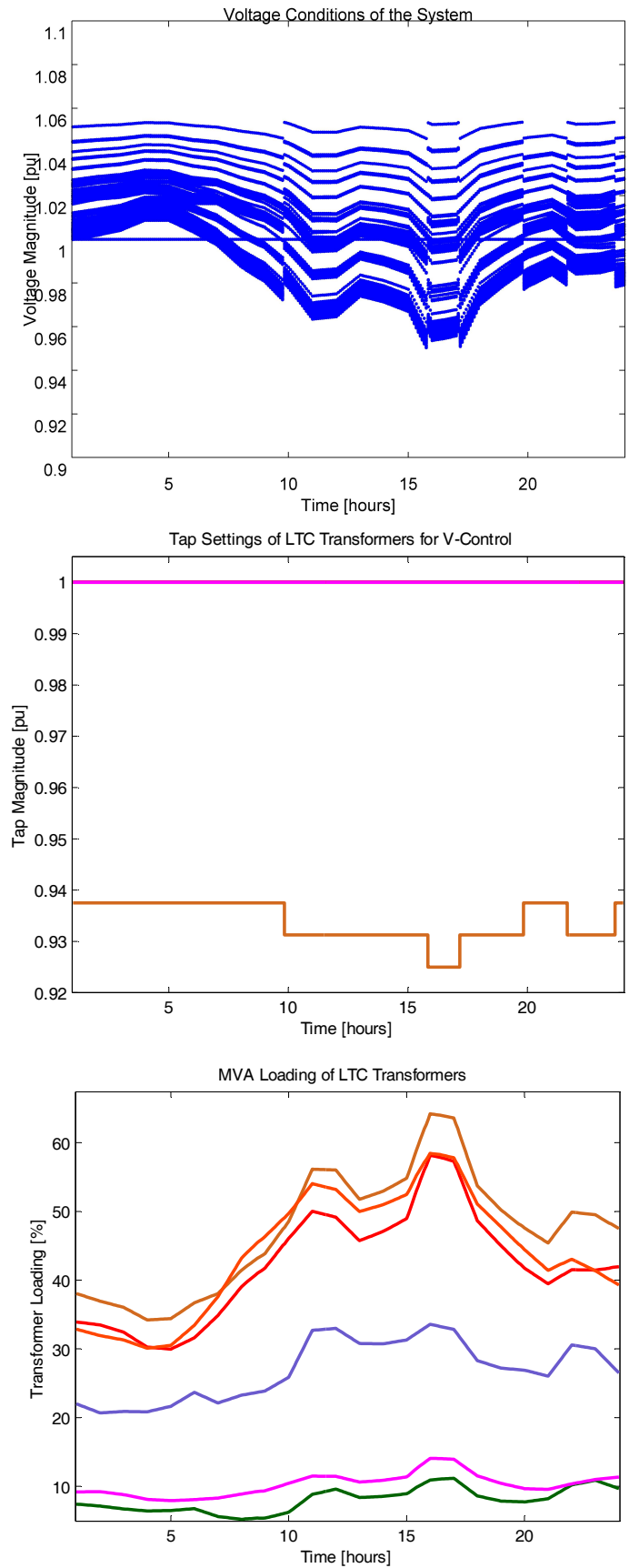


Figure 12 – Standard operation of the system - voltage control using the 115/4.16 kV transformer: voltage conditions, tap settings, HV/MV and MV/MV transformer loadings

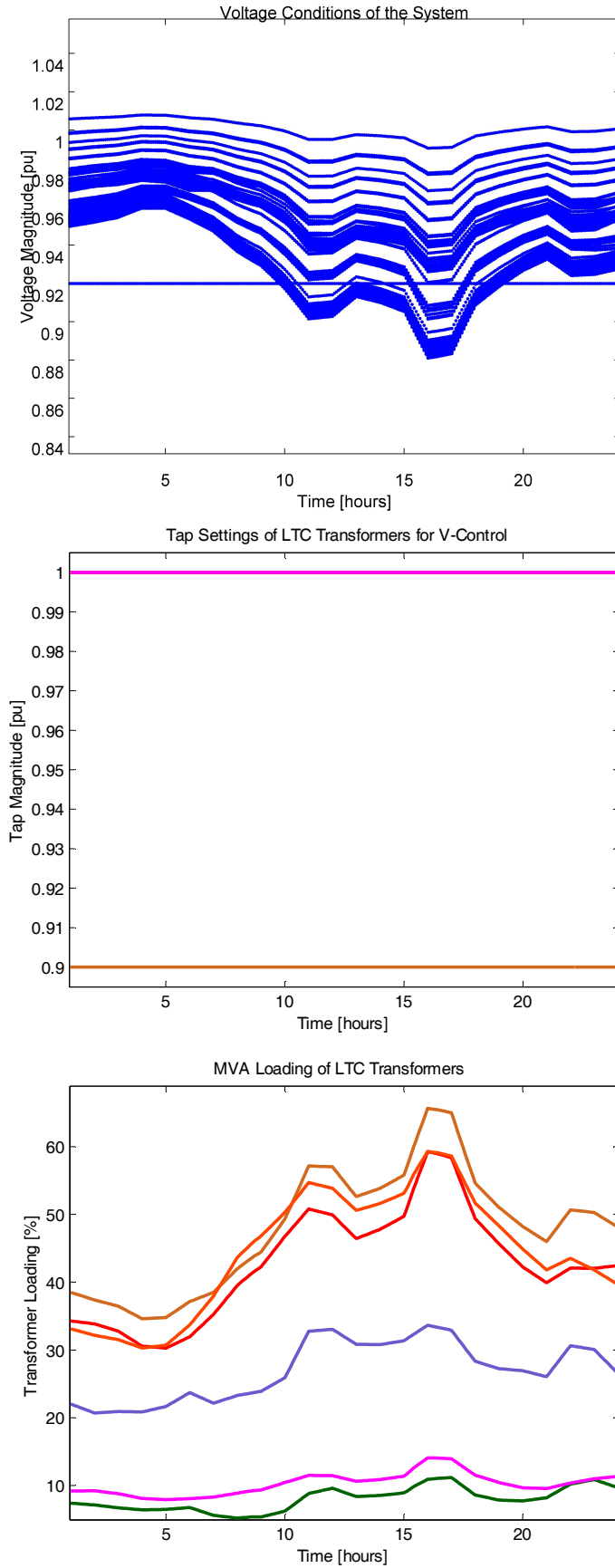


Figure 13 – Abnormal operation of the system - voltage control using the 115/4.16 kV transformer: voltage conditions, tap settings, HV/MV and MV/MV transformer loadings

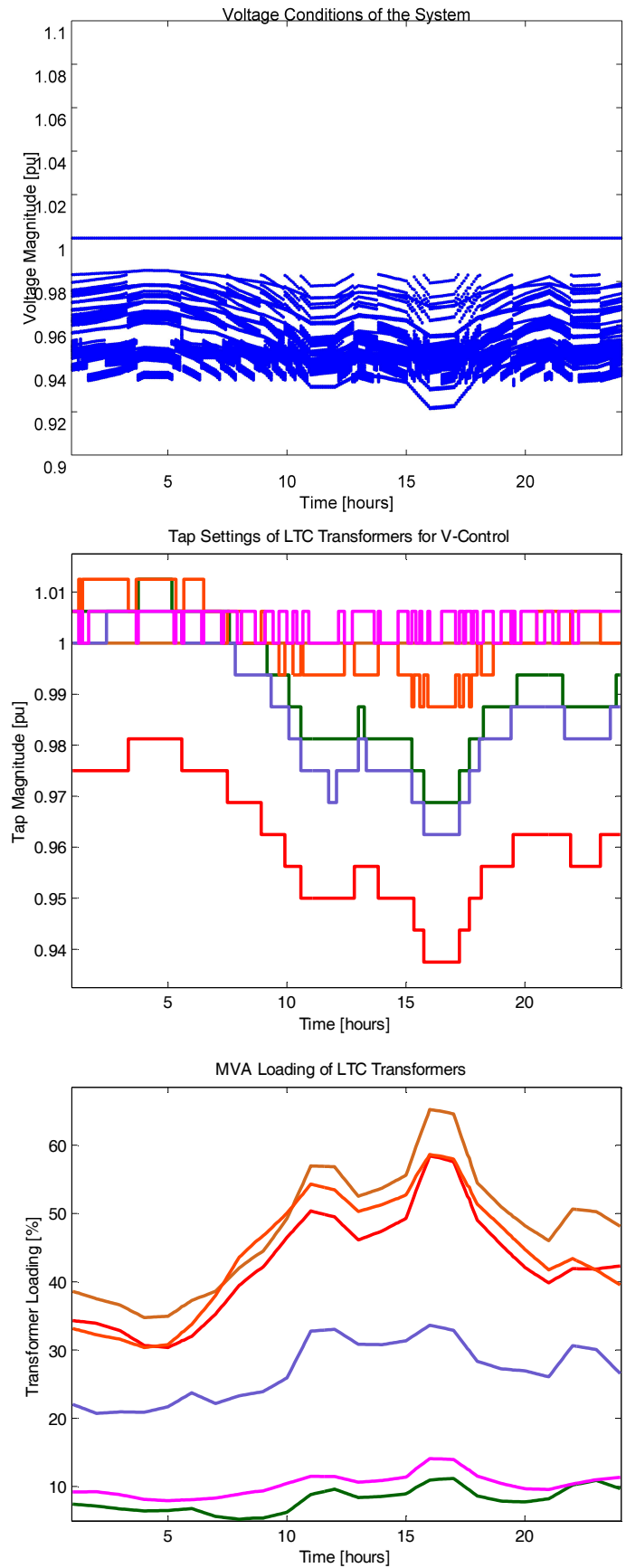


Figure 14 – Standard operation of the system - voltage control using the 4.16/4.16 kV transformers: voltage conditions, tap settings, HV/MV and MV/MV transformer loadings

Therefore, the last simulation was created to show another possible concept with setting the 115/4.16 kV transformer to be with fixed tap setting while remaining MV/MV transformers equipped by on-load tap changers with target voltage values of 0.98 (buses 13-117), 0.95 (buses 18-21, 18-124, 60-118) and 0.94 (buses 97-120) pu. As can be seen in Fig. 14, the voltages have been successfully maintained within the limits but by producing increased number of tap changes during the specified time period. From numerical point of view, high number of load flow cases required more than 14,000 iterations to converge. Total CPU time of this simulation was approx. 50 minutes.

#### 4. CONCLUSIONS

In this paper, voltage control of modified IEEE 123-bus distribution network with 5 photovoltaic power sources has been simulated by total 6 LTC transformers. From the results, superior HV/MV LTC transformer cannot maintain network voltage conditions within their limits in all operational system states. On the contrary, MV/MV LTCs can do so but with very high number of tap changes.

In future work, the Newton-Raphson with corresponding algorithms will be included to provide faster and more reliable solutions. Use of time-variable cloudiness factors will be further tested. As the alternative, inclusion of synchronous condensers (SCs) and capacitor banks for voltage control will be performed. Both studies (SCs and LTCs) will be provided also for the islanded distribution system.

#### REFERENCES

- [1] C.A. Gross, "Power System Analysis - 2<sup>nd</sup> edition", John Wiley & Sons, 1986.
- [2] Soukup, M.: Řízení provozu mikro-sítí napájených OZE - thesis, FEL ZČU Plzeň, 2006.
- [3] Ptáček, M., Matoušek, A.: Modelling of Photovoltaic Array for Hybrid System, EPE conference, VŠB - TU Ostrava, Dlouhé Stráně, 2011.
- [4] Prokop, L., Misak, S.: Hodnocení provozu fotovoltaické elektrárny, EPE conference, VŠB - TU Ostrava, Dlouhé Stráně, 2011.
- [5] Distribution Test Feeders: <http://ewh.ieee.org/soc/pes/dsacom/testfeeders/>, avail. on 11<sup>th</sup> Dec. 2011.
- [6] Photovoltaic Geographical Information System - Interactive Maps: <http://re.jrc.ec.europa.eu/pvgis/apps4/pvest.php#>, avail. on 30<sup>th</sup> Oct. 2011.
- [7] Company OTE, a.s.: <http://www.ote-cr.cz/>, avail. on 3<sup>rd</sup> Jan. 2012.

#### ACKNOWLEDGEMENT

This work has been supported by Technology Agency of the Czech Republic (TACR) project No. TA01020865 and by student science project SGS-2012-047.

#### Author:

Ing. Jan Veleba  
University of West Bohemia in Pilsen  
Department of Electric Power Engineering and Environmental Engineering  
Univerzitní 8, 306 14 Pilsen, Czech Republic  
E-mail: [jveleba@kee.zcu.cz](mailto:jveleba@kee.zcu.cz)  
Tel.: +420 37 763 4314